Inorganic Chemistry

Article

pubs.acs.org/IC

Synthesis and Characterization of an Azido-Bridged Dinuclear Ruthenium(II) Polypyridylamine Complex Forming a Mixed-Valence State

Misaki Makino, Tomoya Ishizuka, Shingo Ohzu, Jiang Hua, Hiroaki Kotani, and Takahiko Kojima*

Department of Chemistry, Graduate School of Pure and Applied Sciences, University of Tsukuba, 1-1-1 Tennoudai, Tsukuba, Ibaraki 305-8571, Japan

Supporting Information

ABSTRACT: We have synthesized a mononuclear ruthenium(II) azido complex (**1**) and a dinuclear ruthenium(II) μ-azido complex (**2**) having *N*,*N*-bis(2-pyridylmethyl)-*N*-bis(2-pyridyl)methylamine (N4Py) as a pentadentate ancillary ligand. In the crystal structure of **2**, intramolecular $\pi-\pi$ stacking was found between the pyridine rings of the two different N4Py ligands, contributing to stabilize the dinuclear μ-azido structure. π donation from the HOMO π^* orbital of the μ-azido ligand to the Ru−N(pyr) bond increases the bond order between the terminal and central N atoms in the μ-azido ligand to strengthen the N−N bonds of the μ-azido ligand. The μ-azido complex **2** was revealed to exhibit a stepwise oxidation behavior in CH_3CN to afford a $Ru^{II}-\mu$-azido$-Ru^{III}$ mixed-valence (MV) state upon one-electron oxidation. The MV state of one-electron-oxidized **2** was categorized in the Robin−Day class II with the electronic coupling constant (H_{ab}) of 570 cm^{-1}.

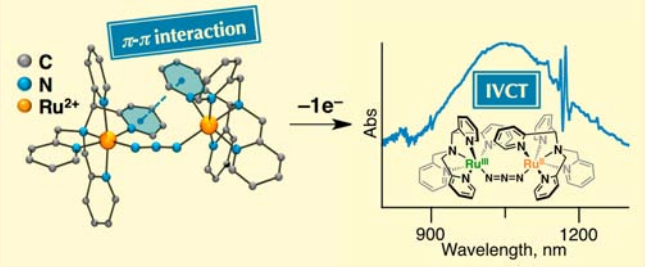

INTRODUCTION

Transition-metal complexes showing a mixed-valence (MV) state,[1] represented by the Creutz−Taube ion,[2] have attracted considerable attention not only as model compounds for studies on intramolecular electron transfer (ET)[3,4] but also for functional dyes and materials such as Prussian blue.[5,6] The MV compounds were categorized by Robin and Day into three classes depending on the strength of the electronic interaction between the donor and acceptor sites.[7] The class I compounds show no electronic interaction, whereas in class III, the two redox-active metal centers are no longer discernible because of the strong interaction and the charge was fully delocalized to give a partial valence state on the two metal centers, respectively. Class II is recognized as the intermediate situation of the former two classes. To date, a lot of efforts have been made to clarify the effect of the distance between two redox sites on the electronic interaction, the ability of the bridging ligand to delocalize the charge, and the role of the coordination environment of the metal centers in controlling the ET rate.[8] Recently, the effects of the anionic bridging ligands on the MV properties have been investigated in detail.[9,10] In addition, besides dinuclear ruthenium complexes, MV complexes of other metals[11] and pure organic MV systems[12] have also attracted considerable attention.

As a bridging ligand, an azide ion (N_3^-) has been also intensively studied for constructing molecular magnets[13,14] and low-dimensional magnets.[15] The μ-azido ligand exhibits two kinds of coordination modes: end-on type (μ-1,1-N_3) and end-to-end type (μ-1,3-N_3) (Chart 1).[16] Despite the unique coordination behavior of the μ-azido ligand and the outstanding properties for mediating the magnetic properties of the metal centers as mentioned above, the electronic conduction properties of a μ-azido ligand for delocalizing the charge in MV compounds have been rarely investigated.[17] In particular, the ruthenium complexes with μ-azido ligands reported so far are limited for end-on-type bis(μ-azido) complexes[18] and end-to-end-type bis(μ-azido) complexes,[19] and the electrochemical properties have yet to be well investigated.[20] Herein, we synthesized an end-to-end dinuclear ruthenium(II) μ-azido complex, **2**, and investigated the electrochemical properties in

Chart 1. Coordination Modes of the μ-Azido Ligand

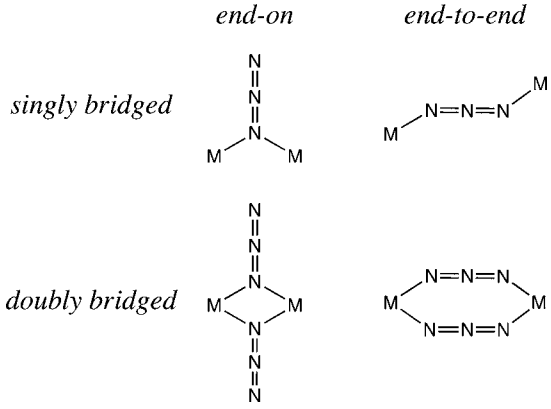

Received: February 18, 2013
Published: April 22, 2013

   dx.doi.org/10.1021/ic400412f | Inorg. Chem. 2013, 52, 5507−5514

Scheme 1. Synthesis of 1 and 2

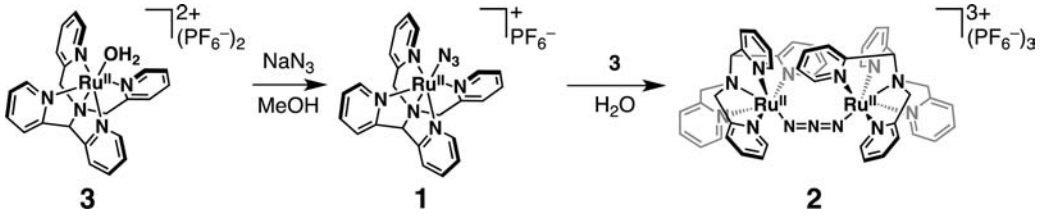

CH_3CN. We found that complex **2** exhibits stepwise one-electron-oxidation behavior to afford a MV state, Ru^{II}–μ-azido–Ru^{III}, by chemical oxidation.

EXPERIMENTAL SECTION

General Procedures. Chemicals and solvents were used as received from Tokyo Chemical Industry Co., Wako Chemicals, or Sigma-Aldrich Corp. unless otherwise mentioned. UV–vis spectra were obtained on a Shimadzu UV-3600 spectrophotometer. Syntheses of *N*,*N*-bis(2-pyridylmethyl)-*N*-bis(2-pyridyl)methylamine (N4Py),[21] $[Ru^{II}Cl(N4Py)](PF_6)$,[22] and $[Ru^{II}(N4Py)(OH_2)](PF_6)_2$ (**3**)[23] were conducted with the reported procedure. ^{1}H NMR spectra were recorded on JEOL EX-270 and Bruker AV400 spectrometers in $CDCl_3$ (deuteration percentage: 99.8%) and acetone-d_6 (deuteration percentage: 99.9%) at room temperature, and the chemical shifts were determined using the residual solvent peak as a reference. Electrospray ionization mass spectrometry (ESI-MS) spectra were recorded on a JEOL AccuTOF CS JMS-T100CS mass spectrometer in acetone or MeOH. Electrochemical measurements were performed on a BAS CV-1B voltammetric analyzer in purified CH_3CN in the presence of 0.1 M $[(n\text{-}Bu)_4N]PF_6$ as an electrolyte under argon at room temperature or at −40 °C with a platinum disk as the working electrode, a platinum wire as the counter electrode, and Ag/AgCl as the reference electrode. Ferrocene was used as a standard to determine the redox potentials. IR spectra were recorded on a Jasco FT/IR-4100 spectrometer with a standard KBr method.

Synthesis. *$[Ru^{II}(N_3)(N4Py)](PF_6)$ (**1**).* A solution containing **3** (30 mg, 0.039 mmol) and NaN_3 (3.0 mg, 0.039 mmol) in MeOH (20 mL) was degassed by three freeze–pump–thaw cycles and stirred for 1 h at room temperature in the dark. The solution color changed from yellow to red. MeOH was removed under reduced pressure, and the residual solid was dissolved in tetrahydrofuran (THF). For recrystallization, chilled hexane was added slowly to the THF solution of **1** and the red crystals obtained were filtered and dried in vacuo. Yield: 16.4 mg (60%). ^{1}H NMR (acetone-d_6): δ 4.65 (s, 4H, NCH_2Py), 6.83 (s, 1H, $NCHPy_2$), 7.15 (d, J = 7.8 Hz, 2H, H3 of $PyCH_2N$), 7.40 (dd, J = 7.8 and 5.6 Hz, 2H, H5 of $PyCH_2N$), 7.48 (ddd, J = 7.4, 5.5, and 2.0 Hz, 2H, H5 of Py_2CHN), 7.67 (td, J = 7.8 and 1.6 Hz, 2H, H4 of $PyCH_2N$), 8.00 (td, J = 7.4 and 1.6 Hz, 2H, H4 of Py_2CHN), 8.07 (dd, J = 7.4 and 2.0 Hz, 2H, H3 of Py_2CHN), 9.02 (dd, J = 5.5 and 1.6 Hz, 2H, H6 of Py_2CHN), 9.10 (dd, J = 5.6 and 1.6 Hz, H6 of $PyCH_2N$). ESI-MS (MeOH): m/z 511.1 ($[M - PF_6]^+$). UV–vis (MeCN): λ_{max} 467, 379, 246 nm. IR (KBr): ν 2024 cm^{-1} (N_3). The sample of **1** for elemental analysis was prepared through recrystallization with vapor diffusion of octane to the CH_2Cl_2 solution. Anal. Calcd for $C_{23}H_{21}N_8RuPF_6 \cdot 0.25CH_2Cl_2$: C, 41.27; H, 3.20; N, 16.60. Found: C, 41.57; H, 3.35; N, 16.60.

*$[\{Ru^{II}(N4Py)\}_2(\mu\text{-}N_3)](PF_6)_3$ (**2**).* A solution containing **1** (10.8 mg, 0.015 mmol) and **3** (12 mg, 0.015 mmol) in H_2O (30 mL) was heated at 30–40 °C for 3 h. The solution was concentrated, and a saturated aqueous solution of KPF_6 was added. The red precipitate formed was filtered and recrystallized from acetone/hexane. The resulting bright-red crystals were filtered and dried in vacuo. Yield: 15.6 mg (71%). ^{1}H NMR (acetone-d_6): δ 4.67 (ABq, J_{AB} = 18 Hz, 4H, NCH_2Py), 6.84 (ddd, J = 7.8, 5.4, and 1.6 Hz, 2H, H5 of Py_2CHN), 6.87 (s, 1H, $NCHPy_2$), 7.20 (d, J = 7.7 Hz, 2H, H3 of $PyCH_2N$), 7.43 (dd, J = 7.7 and 5.6 Hz, 2H, H5 of $PyCH_2N$), 7.74 (td, J = 7.7 and 1.2 Hz, 2H, H4 of $PyCH_2N$), 7.91 (td, J = 7.8 and 1.2 Hz, 2H, H4 of Py_2CHN), 8.12 (dd, J = 7.8 and 1.6 Hz, 2H, H3 of Py_2CHN), 8.63 (dd, J = 5.4 and 1.2 Hz, 2H, H6 of Py_2CHN), 9.17 (dd, J = 5.6 and 1.2 Hz, H6 of $PyCH_2N$). ESI-MS (acetone): m/z 1270.3 ($[M - PF_6]^+$). UV–vis (MeCN): λ_{max} 450, 366, 246 nm. IR (KBr): ν 2040 cm^{-1} (N_3). Anal. Calcd for $C_{46}H_{42}N_{13}Ru_2P_3F_{18}$: C, 39.07; H, 2.99; N, 12.88. Found: C, 39.13; H, 2.88; N, 12.64.

X-ray Crystallography on 1 and 2. The crystals of **1** and **2** were mounted on a mounting loop with epoxy resin. All measurements were performed on a Bruker APEXII diffractometer at −153 °C with graphite-monochromated Mo Kα radiation (λ = 0.71073 Å). The data were collected up to 2θ = 55.0°. The structures were solved by direct methods and expanded using Fourier techniques. All non-H atoms were refined anisotropically, and the refinement was carried out with full-matrix least squares on F. All calculations were performed using the Yadokari-XG crystallographic software package,[24] and structure refinements were made using *SHELX-97*.[25] Crystallographic data for **1**: $C_{23}H_{21}N_8Ru \cdot PF_6$, fw = 655.52, red, triclinic, space group $P\bar{1}$, cell parameters a = 13.4461(13) Å, b = 14.5506(14) Å, c = 16.7938(16) Å, α = 73.8770(10)°, β = 89.4520(10)°, γ = 84.8560(10)°, V = 3143.3(5) Å^3, T = 120(2) K, Z = 4, D_c = 1.385 g cm^{-3}, 17868 reflections measured, 13576 unique (R_{int} = 0.0228), $R1$ = 0.0463 [$I > 2\sigma(I)$] and $wR2$ = 0.1146 (all reflections), GOF = 1.034. Crystallographic data for **2**: $C_{46}H_{42}N_{13}Ru_2 \cdot 3PF_6$, fw = 1413.98, red, orthorhombic, space group $I2_12_12_1$, cell parameters a = 12.914(4) Å, b = 13.120(4) Å, c = 39.995(13) Å, V = 6776(4) Å^3, T = 120(2) K, Z = 4, D_c = 1.386 g cm^{-3}, 17379 reflections measured, 6864 unique (R_{int} = 0.0689). $R1$ = 0.0988 [$I > 2\sigma(I)$] and $wR2$ = 0.2593 (all reflections), GOF = 1.039. In both cases, highly disordered CH_2Cl_2 and acetone molecules as the solvent molecules of crystallization were deleted using the *SQUEEZE* program.[26]

RESULTS AND DISCUSSION

Synthesis of Mononuclear Ruthenium(II) Azido and Dinuclear Ruthenium(II) μ-Azido Complexes. A mononuclear ruthenium(II) azido complex (**1**), having N4Py[21] as an ancillary ligand, was synthesized by using **3**[23] as the starting material. The synthetic procedure is summarized in Scheme 1. Complex **3** was treated with NaN_3 in MeOH at room temperature, and after evaporation of the solvent, the residual solid was recrystallized from THF/hexane to give wine-red crystals of **1** in 60% yield. The ^{1}H NMR spectrum of **1** in acetone-d_6 showed a spectral pattern reflecting the C_s symmetry of **1**, including eight aromatic proton signals assignable to those of the two types of pyridine rings in the range of δ 7.0–9.2 ppm (Figure 1a). The ^{1}H NMR signals assigned to the methine and methylene protons were observed at δ 6.83 (s) and 4.65 (s) ppm, respectively, and the chemical shifts were comparable to those of the corresponding signals of **3** in acetone-d_6 [δ 6.89 ppm (s) for the methine proton and δ 4.63 and 4.75 ppm (ABq) for the methylene protons].[23] The methylene protons of **1** showed a singlet ^{1}H signal in contrast to the case of **3**. In the ESI-TOF-MS (where TOF = time-of-flight) spectrum of **1** in MeOH, a peak cluster with the biggest peak at m/z 511.1 was observed and the isotopic pattern was well matched with the simulated one for the $[Ru^{II}(N_3)(N4Py)]^+$ ion [Figure S1 in the Supporting Information (SI)].

dx.doi.org/10.1021/ic400412f | Inorg. Chem. 2013, 52, 5507–5514

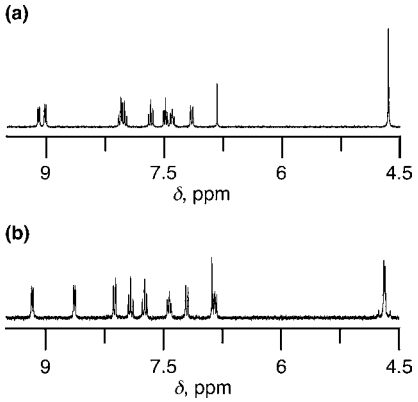

Figure 1. ^{1}H NMR spectra of **1** (a) and **2** (b) in acetone-d_6.

The synthesis of an azido-bridged dinuclear ruthenium(II) complex, **2**, was done by condensation with **1** and **3** in H_2O at 30−40 °C (Scheme 1). The addition of an excess amount of KPF_6 to the reaction mixture afforded a red powder of **2**. In the ^{1}H NMR spectrum of **2** in acetone-d_6, two sets of four signals ascribed to two types of 2-substituted pyridine rings were observed as in the case of **1** (Figure 1b). The assignment of each signal was done on the basis of the 2D ^{1}H−^{1}H COSY spectrum and the 1D differential NOE spectrum (Figures S2 and S3 in the SI). The two ^{1}H signals at the 5 and 6 positions of the pyridine rings linked with the methine carbon for **2** appeared at δ 6.84 and 8.63 ppm, respectively, and exhibited upfield shifts relative to the corresponding signals for **1** [δ 7.48 (H5) and 9.02 (H6) ppm]. In contrast, the ^{1}H signals of the protons at the 3 and 4 positions of the pyridine rings linked with the methine carbon and those of all of the protons of the pyridine rings linked with methylene carbons for **2** were observed at positions similar to those of the corresponding signals for **1**. This indicates that the intramolecular $\pi-\pi$ stacking between the pyridine rings linked with the methine carbons of the two N4Py ligands and the resulting ring-current effects caused the upfield shifts of the 5 and 6 proton signals of the methine-bridged pyridines in **2**. The intramolecular $\pi-\pi$ stacking was also observed in the crystal structure of **2** (vide infra). The ESI-MS spectrum of **2** in acetone gave two peak clusters ascribed to the parent signal due to $\{[\{Ru^{II}(N4Py)\}_2(\mu\text{-}N_3)](PF_6)_2\}^+$ at m/z 1270.3 and the fragment signal ascribed to $[Ru^{II}(N_3)(N4Py)]^+$ at m/z 511.1 (Figure S1b in the SI).

Crystal Structures of 1 and 2. A single crystal of **1** suitable for X-ray diffraction analysis was obtained by recrystallization from CH_2Cl_2/octane. Complex **1** was crystallized into a triclinic lattice with space group $P\bar{1}$. The asymmetric unit included two independent molecules of the cation part of **1** (Figure 2a), two PF_6^- ions as the counteranions, and four highly disordered CH_2Cl_2 molecules, which were thus deleted using the *SQUEEZE* program.[26] Complex **2** was recrystallized with vapor diffusion of hexane to the acetone solution to obtain a single crystal, which was suitable for X-ray crystallography. Complex **2** was crystallized into an orthorhombic lattice with space group $I2_12_12_1$. In the asymmetric unit were included half of the cation part of **2** (Figure 2b) and one and a half of the PF_6 ions. Two acetone molecules were also cocrystallized, but highly disordered, and thus deleted with use of the *SQUEEZE* program.[26] The selected bond lengths of **1** and **2** in the crystal structures are summarized in Table 1.

Table 1. Selected Bond Lengths (Å) of 1 and 2

	1		2
Ru−N1	2.039(3)	2.030(3)	2.022(10)
Ru−N2	2.058(3)	2.049(3)	2.011(10)
Ru−N3	2.043(3)	2.058(3)	2.067(8)
Ru−N4	2.053(3)	2.051(3)	2.056(10)
Ru−N5	2.065(3)	2.046(3)	2.057(8)
Ru−N6	2.158(3)	2.122(3)	2.121(10)
N6−N7	1.138(5)	1.181(4)	1.103(9)
N7−N8	1.172(6)	1.171(5)	

The bond lengths between the central metal and the end N atom of the azido ligand (Ru−N6) for both **1** and **2** are in the typical range of those of reported ruthenium(II) complexes with similar coordination environments.[18,19] In a comparison of the Ru−N1 bond lengths of **1** to those of other Ru^{II}N4Py complexes, $[Ru^{II}Cl(N4Py)](PF_6)$,[22] **3**,[23] $[Ru^{II}(ClO_4)(N4Py)](PF_6)$ (Figure S4a in the SI),[27] and $[Ru^{II}(N4Py)(NCCH_3)](PF_6)_2$ (Figure S4b[27] and Table S1 in the SI), the order is $[Ru^{II}Cl(N4Py)]^+$ [Ru−N1 = 2.036(3) Å] ∼ **1** (2.035 Å)[28] > $[Ru^{II}(N4Py)(NCCH_3)]^{2+}$ (2.014 Å)[28] ∼ $[Ru^{II}(ClO_4)(N4Py)]^+$ [2.009(4) Å] > **3** [1.968(5) Å]. This tendency can be explained on the basis of the strength of the σ-donating ability of the axial ligand, and the order matches the strength of the trans effects by the axial ligands reported in the literature [Cl^- > N_3^- (>ClO_4^-) > H_2O].[29,30] The N−N bond lengths of the end-on azido ligands in **1** were 1.160 Å for N6−N7[28] and 1.172 Å for N7−N8,[28] and were in the range of values for similar ruthenium(II) azido complexes reported so far.[31] In contrast, the N6−N7 bond distance of the μ-azido ligand in **2** [1.103(9)

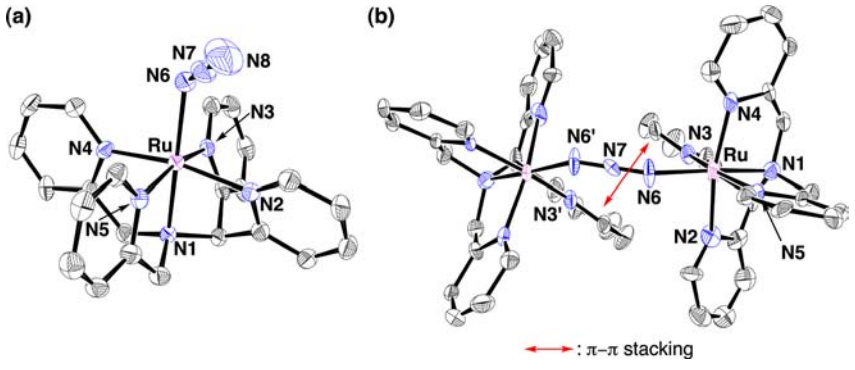

Figure 2. Crystal structures of the cation parts of **1** (a) and **2** (b). The thermal ellipsoids are drawn with 50% probability.

dx.doi.org/10.1021/ic400412f | Inorg. Chem. 2013, 52, 5507−5514

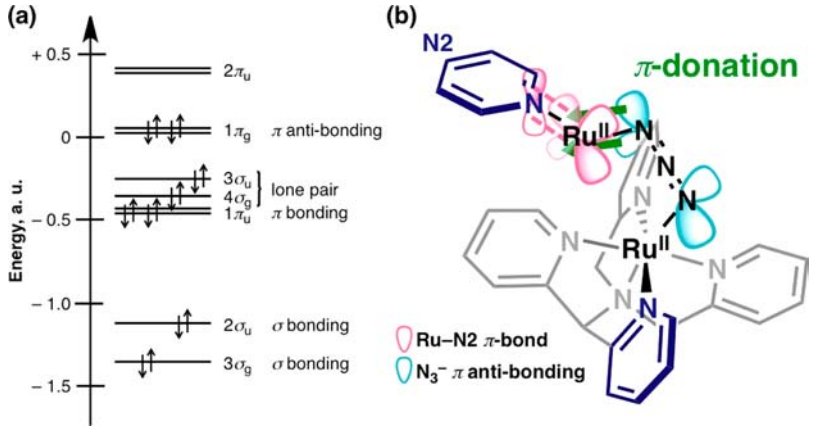

Figure 3. (a) Molecular orbitals of the N_3^- ion[33] and (b) schematic description of π donation from the azido ligand to the Ru−N2 bond.

Å] is much shorter than those of **1** and other metal−N_3 complexes (mean value, 1.17 Å)[14,15,18,19,31] and even shorter than those of free N_3^- ions (1.17−1.19 Å).[32] This can be explained by the fact that the doubly degenerated highest occupied molecular orbitals (HOMOs) of the N_3^- ion are slightly antibonding π-type orbitals ($1\pi_g$),[33] and thus reduction of the electron density on the HOMO π^* orbitals of N_3^- by donation to the two Ru^{II} moieties causes a shortening of the N−N bonds in the μ-azido ligand. The resultant enhancement of π-back-bonding from the Ru^{II} center to the pyridine ring including N2 makes the bond length of Ru−N2 of **2** [2.011(10) Å] relatively shorter compared to those of other Ru−N(pyr) bonds (the mean value is 2.06 Å). Closely looking over the crystal structure of **2**, the terminal nitrogen (N6) of the μ-azido ligand was forced to come close to the N2 atom with a N2···N6 distance of 3.03(1) Å by the intramolecular π−π stacking between N3− and N3′−pyridine rings (Figure S5 in the SI). Consequently, the occupied π^* orbitals ($1\pi_g$) of the μ-azido ligand direct toward the π orbital of the Ru−N2 bond and thus π donation from the azido ligand to the Ru−N2 π bond is likely to occur (Figure 3), which clearly matches the explanation for the short N−N bond length of the μ-azido ligand in **2** mentioned above. In contrast, the mononuclear azido complex **1**, lacking such an intramolecular π−π stacking force (vide infra), did not exhibit shortening of the N−N bond of the azido ligand or of the Ru−N(pyr) bonds. Supporting this, the N_3 stretching band of **2** was observed at 2040 cm^{-1}, showing a high-energy shift relative to that of **1** [$\nu(N_3)$ = 2024 cm^{-1}; see Figure S6 in the SI].[34] This result also indicates reinforcement of the N−N bonds in the μ-azido ligand of **2**. Dinuclear μ-azido complexes with second- and third-row transition-metal ions reported so far have shown a tendency to undergo thermal and photochemical decomposition of the μ-azido ligand to give nitrido or μ-nitrido complexes and their derivatives,[17,35] hampering a detailed investigation of the redox properties of the μ-azido complexes. In contrast, the strengthened μ-azido ligand of **2** enabled the electrochemical studies of **2** to elucidate the characteristics of the MV state (vide infra).

The pyridine moieties including N3 and N3′ of **2** formed intramolecular π−π stacking with a distance of 3.34 Å in the crystal structure. This π−π stacking probably plays a role in stabilizing the dimeric structure.[36] The effects of intramolecular π−π stacking were also observed in the ^{1}H NMR spectrum of **2** as upfield shifts of the protons at the 5 and 6 positions of the pyridine rings (vide supra), but the two pyridine rings linked to the methine carbon (N2 and N3 pyridines in the crystal structure) were equivalent in the ^{1}H NMR spectrum at least at room temperature. This indicates that the intramolecular π−π-stacked pyridine rings (N3 pyridine in the crystal structure) show a fast-flipping motion to exchange positions with the other pyridines (N2 pyridine) in solution.

Redox Properties and MV State of 2. The cyclic voltammogram (CV) of **1** in CH_3CN exhibited a reversible wave at $E_{1/2}$ = +0.50 V vs SCE, which can be assigned to the redox process of the Ru center (Ru^{II}/Ru^{III}; Figure 4a). The

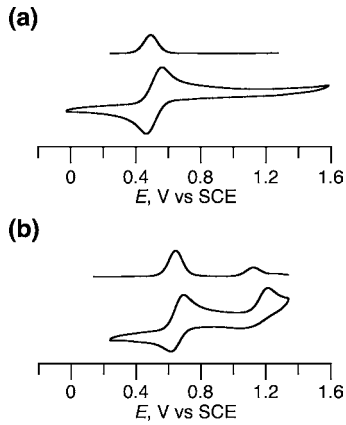

Figure 4. CVs (below) and DPVs (above) of **1** (a) and **2** (b) in CH_3CN in the presence of $[(n\text{-}Bu)_4N](PF_6)$ as an electrolyte at room temperature. Scan rate: 0.2 V s^{-1}.

redox potential was relatively low compared to those of other polypyridyl-type Ru−N_6 complexes having anionic ligands with extended π-conjugated systems.[37] The reason for the low redox potential of **1** is the strong σ donation of the tertiary amine N atom of the N4Py ligand[38] and the weak π acceptability of the monomeric pyridine rings compared to the π-conjugated polypyridyl rings. On the other hand, in the CV of **2** in CH_3CN at room temperature were observed a reversible wave at $E_{1/2}$ = +0.65 V vs SCE and a quasi-reversible wave at E_{pa} = +1.26 V and E_{pc} = +1.08 V vs SCE,[39] whose potential was determined as +1.13 V vs SCE with a differential pulse voltammogram (DPV; Figure 4b). The first redox potential for **2** was slightly higher than that of **1**, which indicates the smaller σ donation of the μ-azido ligand due to the bridging of the two cationic metal centers. The two processes are supposed to be derived from the redox processes of Ru^{II}−Ru^{II}/Ru^{II}−Ru^{III} and

dx.doi.org/10.1021/ic400412f | Inorg. Chem. 2013, 52, 5507−5514

Ru^{II}–Ru^{III}/Ru^{III}–Ru^{III}, respectively. Thus, the former oxidation process can afford the one-electron-oxidized species of **2** ($\mathbf{2^{ox}}$) in a Ru^{II}–Ru^{III} MV state. The low reversibility of the second redox wave for **2** should probably be not caused by the instability of the MV Ru^{II}–Ru^{III} state but by that of the Ru^{III}–Ru^{III} state.

To confirm the formation of the MV state, we oxidized **2** with tris(4-bromophenyl)ammoniumyl hexachloroantimonate (TBAH; E = +1.07 V vs SCE)[40] in CH_3CN at room temperature and monitored the change with the optical absorption spectra (Figure 5b). Then, the two metal-to-ligand

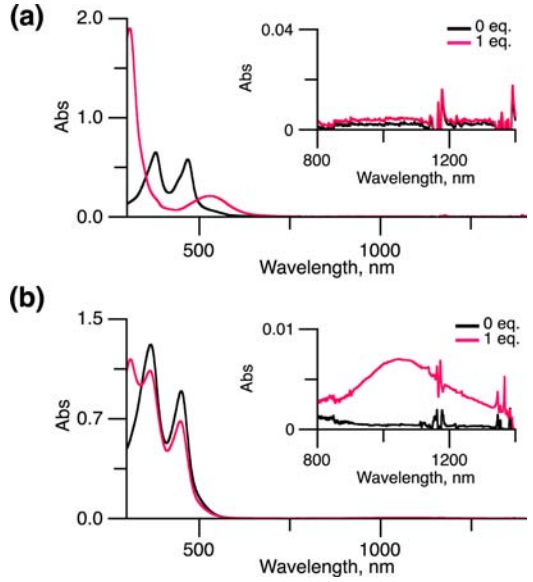

Figure 5. (a) Absorption spectra of **1** (black line) and one-electron-oxidized species of **1** (red line) in CH_3CN at −40 °C. (b) Absorption spectra of **2** (black line) and one-electron-oxidized species of **2** (red line) in CH_3CN at room temperature. The one-electron-oxidized forms of **1** and **2** were formed in situ by the addition of 1 equiv of TBAH.

charge-transfer (MLCT) absorption bands of **2** at 450 and 366 nm, which are assigned to CT transitions from the Ru^{II} centers to the μ-azido ligand[41] and that to the pyridine rings of the N4Py ligands,[23] respectively, were decayed upon addition of the oxidant (Figure S8 in the SI). At the moment upon the addition of 1 equiv of the oxidant, the MLCT bands based on the Ru^{II} center still remained. As strong evidence to support the formation of the MV state, the intervalence charge-transfer (IVCT) band was observed at 1050 nm (ε = 140 M^{-1} cm^{-1}) upon the addition of 1 equiv of the oxidant (Figure 5b), and the absorption band almost disappeared upon the addition of 2 equiv of the oxidant.[42] For evidence that the long-wavelength absorption band was not simply derived from the Ru^{III} species, we also measured the UV–vis spectra of one-electron-oxidized species of **1** in CH_3CN at −40 °C (Figure 5a). The UV–vis spectra of one-electron-oxidized **1** showed decay of the two MLCT absorption bands at 467 and 379 nm, corresponding to the absorption bands observed for **2**, respectively, and a new band appeared at 529 nm, which can be assigned to the ligand-to-metal charge-transfer transition from the azido ligand to the Ru^{III} centers formed by the oxidation.[43] This spectral change of **1** upon oxidation resembles to that of **2** in the UV–vis region (300–700 nm). On the other hand, the near-IR absorption band, ascribable to the IVCT transition, was not observed for **1** upon one-electron oxidation.

The comproportionation constant (K_C) of the MV state of $\mathbf{2^{ox}}$ at 298 K was estimated to be 4.4 × 10^8, with the difference between the first and second oxidation potentials (ΔE [mV]) based on eq 1, which indicates the relatively large stability of the MV state.

$$K_C = 10^{\Delta E/59\ \mathrm{mV}} \text{ at } 298\ \mathrm{K} \quad (1)$$

In addition, the electronic coupling parameter (H_{ab}) of $\mathbf{2^{ox}}$ was calculated as 570 cm^{-1}, according to the Hush equation, as indicated in eq 2:[44,45]

$$H_{ab} = 0.0206(\varepsilon_{max}\nu_{max}\Delta\nu_{1/2})^{1/2}/r_{ab} \quad (2)$$

Here, ε_{max} is the absorption coefficient of the IVCT transition, ν_{max} is the energy (cm^{-1}) of the absorption maxima of the IVCT band, $\Delta\nu_{1/2}$ is the observed full width at half-maximum of the IVCT band, and r_{ab} is the distance between the two Ru^{II} centers [5.602(2) Å] based on the crystal structure of **2**. The Γ parameter, introduced by Sutin and co-workers,[1b] was determined for the IVCT band to be 0.34, in accordance with eq 3.

$$\Gamma = 1 - \Delta\nu_{1/2,exp}/\Delta\nu_{1/2,theo} \quad (3)$$

These IVCT parameters indicate that the MV state of $\mathbf{2^{ox}}$ should be categorized in the Robin–Day class II,[7] suggesting a partially valence-delocalized situation. To our knowledge, this is the first example of a μ-azido-bridged complex, which is fully investigated on the MV properties to obtain the IVCT parameters. In order to evaluate the CT ability of the μ-azido ligand, we compared the IVCT parameters of $\mathbf{2^{ox}}$ with those of dinuclear ruthenium complexes with various bridging ligands (Figure 6 and Table 2).[1,46–50] Four complexes, **4** and **6**–**8**, listed in Table 2 are categorized into the Robin–Day class III, indicating strong electronic coupling between the two Ru centers.[1,47–49] In particular, a cyanogen-bridged **6**[47] and a dinitrogen-bridged **7**,[48] which have linear bridging ligands similar to the μ-azido ligand for **2**, show very strong electronic interactions between the two Ru centers in the MV states

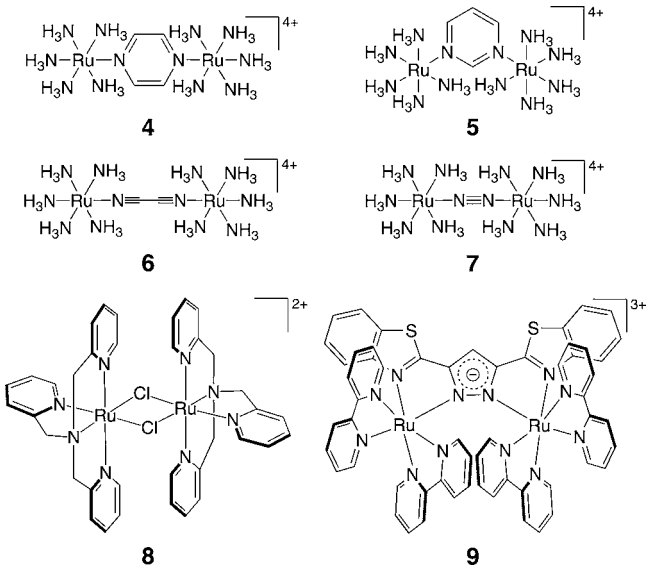

Figure 6. Molecular structures of dinuclear ruthenium complexes showing their MV states.

dx.doi.org/10.1021/ic400412f | Inorg. Chem. 2013, 52, 5507–5514

Table 2. Metal-to-Metal Distances, Absorption Maxima, Widths and Intensities of IVCT Bands, Electronic Coupling Constants, and Comproportionation Constants for MV Complexes Derived from 2 and 4−9

	r_{ab} [Å]	ν_{max} [cm^{-1}]	$\Delta\nu_{1/2}$ [cm^{-1}]	ε_{max} [M^{-1} cm^{-1}]	H_{ab} [cm^{-1}]	Γ	K_C
2	5.6	9500	3060	140	570	0.34	4.4×10^8
4[a]	6.9	6400	1250	5000	3200	0.67	4.0×10^6
5[b]	6.0	7150	6000	41	143	−0.47	343
6[c]	7.7	7000	1610	410	3500	0.60	$>10^{13}$
7[d]	5.0	9800	2630	1400	4900	0.45	10^8
8[e]	3.6	9240	4500	120	4340	0.03	1.6×10^8
9[f]	4.7	10500	5100	110	335	−0.04	2×10^4

[a]Reference 1. [b]Reference 46. [c]Reference 47. [d]Reference 48. [e]Reference 49. [f]Reference 50.

relative to that of $\mathbf{2}^{ox}$, despite the fact that the distances of the two Ru centers are slightly shorter or even longer than that for **2**. This is caused by the difference in the configuration between the Ru centers and the bridging ligands and in the resulting overlapping degree of the atomic orbitals: In the cases of **6** and **7**, the bridging ligand linearly coordinates to the Ru centers, and thus the overlapping of the orbitals mediating the electronic coupling can be maximized, whereas Ru−μ-N_3−Ru in **2** is bent in the *syn* configuration and the overlapping of the orbitals becomes relatively small. On the other hand, the number of intervening atoms between the two Ru centers for complex **5**[46] is three, equal to that of **2**. The distances between the two Ru centers of **2** and **5** (6.0 Å) are similar to each other, whereas the IVCT band of one-electron-oxidized **5** was very weakly observed at 1400 nm in comparison with that of $\mathbf{2}^{ox}$. Reflecting the intense IVCT band of $\mathbf{2}^{ox}$, the IVCT parameters indicated the strong electronic interaction between the two Ru centers via the μ-azido bridge in $\mathbf{2}^{ox}$ in comparison with that in one-electron-oxidized **5**. In addition, a MV state of the one-electron-oxidized species of **9** bridged by a pyrazole derivative as the ligand[50] has been reported to exhibit a weaker electronic coupling between the two Ru centers than that for **2**, despite the fact that the intervening atoms between the two Ru centers in **9** is two, less than that in **2**, and thus the distance between the two Ru centers for **9** (4.7 Å) is shorter than that for **2**. The one-electron-oxidized species of **9** was classified in Robin−Day class II. Therefore, the μ-azido bridge in $\mathbf{2}^{ox}$ mediates relatively well the ET between the donor and acceptor sites, even though it is bent in the *syn* configuration. Despite the large potential splitting and the resultant large K_C, the electronic coupling of **2** was relatively moderate. This can be explained that the asymmetric nature of the μ-azido ligand in $\mathbf{2}^{ox}$,[51] where the anionic charge of the μ-azido ligand is rather localized at the end N atom on the Ru^{III} side by the strong Lewis acidity and the other end N atom on the Ru^{II} side should be rather neutral. Consequently, the formal Ru^{II} center in $\mathbf{2}^{ox}$ becomes electron-deficient, and the redox potential of the $Ru^{II/III}$ couple is positively shifted.

SUMMARY

We synthesized a mononuclear ruthenium(II) azido complex (**1**) and a dinuclear Ru^{II}−μ-azido−Ru^{II} complex (**2**) and characterized the complexes with the use of NMR spectroscopy, MS spectrometry, electrochemical methods, and X-ray crystallography. In the crystal structure of **2**, intramolecular π−π stacking between the pyridine rings of the two different N4Py ligands plays an important role in stabilizing the dinuclear μ-azido structure. π donation from the π^* HOMO orbital of the μ-azido ligand to the Ru−N(pyr) bond may contribute to stabilizing the structure by increasing the bond order between the terminal and central N atoms in the μ-azido ligand. We have also revealed the redox properties of the two complexes: The dinuclear μ-azido complex **2** exhibited a stepwise oxidation behavior: The one-electron oxidation of **2** formed a MV state, where the charge is partially delocalized on the two Ru centers to fall in the Robin−Day class II. The ET properties of MV compounds, whose donor and acceptor centers are bridged by the azido ligand, have yet to be well clarified, whereas herein we have demonstrated the high potential of the μ-azido ligand to mediate ET between the two Ru centers. Other than a mediator of magnetic interaction among paramagnetic metal centers,[52] the properties of a μ-azido ligand as an electronic mediator upon photoexcitation, as exemplified in this study, will provide a basis for the development of new functionality of azido-bridged ruthenium complexes. Further, on the basis of these findings in the work, MV states of ruthenium complexes bridged by other linear anionic ligands such as SCN^- and OCN^-, which are isoelectronic species of N_3^-, can be applied in the scope of the development of a new category of ruthenium complexes, allowing us to observe their MV states.

ASSOCIATED CONTENT

Supporting Information

Crystallographic data of **1**, **2**, $[Ru^{II}(ClO_4)(N4Py)](PF_6)$, and $[Ru^{II}(N4Py)(NCCH_3)](PF_6)_2$ in CIF format, ESI-TOF MS of **1** and **2**, ^1H−^1H COSY and NOE NMR spectra of **2**, ORTEP drawings of $[Ru^{II}(ClO_4)(N4Py)](PF_6)$ and $[Ru^{II}(N4Py)(NCCH_3)](PF_6)_2$, IR spectra of **1** and **2**, CVs, UV−vis spectra, and bond lengths. This material is available free of charge via the Internet at http://pubs.acs.org.

AUTHOR INFORMATION

Corresponding Author

*E-mail: kojima@chem.tsukuba.ac.jp.

Notes

The authors declare no competing financial interest.

ACKNOWLEDGMENTS

This work was supported by Grants-in-Aids 21350035 and 24245011 from the Japan Society of Promotion of Science (JSPS, MEXT) of Japan. T.K. also appreciates financial support from The Asahi Glass Foundation and The Mitsubishi Foundation.

REFERENCES

(1) (a) Demadis, K. D.; Hartshorn, C. M.; Meyer, T. J. *Chem. Rev.* **2001**, *101*, 2655. (b) Brunschwig, B. S.; Creutz, C.; Sutin, N. *Chem. Soc. Rev.* **2002**, *31*, 168. (c) D'Alessandro, D. M.; Keene, F. R. *Chem.*

Rev. **2006**, *106*, 2270. (d) Kaim, W.; Lahiri, G. K. *Angew. Chem., Int. Ed.* **2007**, *46*, 1778.
(2) (a) Creutz, C.; Taube, H. *J. Am. Chem. Soc.* **1969**, *91*, 3988. (b) Creutz, C.; Taube, H. *J. Am. Chem. Soc.* **1973**, *95*, 1086.
(3) (a) Hush, N. S. *Trans. Faraday. Soc.* **1961**, *57*, 557. (b) Hush, N. S. *Electrochim. Acta* **1968**, *13*, 1005.
(4) (a) Hupp, J. T. *J. Am. Chem. Soc.* **1990**, *112*, 1563. (b) Patoux, C.; Launay, J.-P.; Beley, M.; Chodorowski-Kimmes, S.; Collin, J.-P.; Sauvage, J.-P. *J. Am. Chem. Soc.* **1998**, *120*, 3717. (c) Bublitz, G. U.; Laidlaw, W. M.; Denning, R. G.; Boxer, S. G. *J. Am. Chem. Soc.* **1998**, *120*, 6068. (d) Bencini, A.; Ciofini, I.; Daul, C. A.; Ferretti, A. *J. Am. Chem. Soc.* **1999**, *121*, 11418. (e) Salsman, J. C.; Kubiak, C. P.; Ito, T. *J. Am. Chem. Soc.* **2005**, *127*, 2382.
(5) (a) Bernhardt, P. V.; Bozoglián, F.; Macpherson, B. P.; Martínez, M. *Coord. Chem. Rev.* **2005**, *249*, 1902. (b) Sato, O.; Iyoda, T.; Fujishima, A.; Hashimoto, K. *Science* **1996**, *272*, 704.
(6) (a) Ward, M. D. *Chem. Soc. Rev.* **1995**, *34*, 121. (b) Soncini, A.; Mallah, T.; Chibotaru, L. F. *J. Am. Chem. Soc.* **2010**, *132*, 8106. (c) Kobayashi, A.; Kitagawa, H. *J. Am. Chem. Soc.* **2006**, *128*, 12066.
(7) Robin, M. B.; Day, P. *Adv. Inorg. Chem. Radiochem.* **1967**, *10*, 247.
(8) (a) Aguirre-Etcheverry, P.; O'Hare, D. *Chem. Rev.* **2010**, *110*, 4839. (b) Benniston, A. C.; Harriman, A.; Li, P.; Sams, C. A.; Ward, M. D. *J. Am. Chem. Soc.* **2004**, *126*, 13630. (c) Fabre, M.; Bonvoisin, J. *J. Am. Chem. Soc.* **2007**, *129*, 1434.
(9) (a) Gagliardo, M.; Amijs, C. H. M.; Lutz, M.; Spek, A. L.; Havenith, R. W. A.; Hartl, F.; van Klink, G. P. M.; van Koten, G. *Inorg. Chem.* **2007**, *46*, 11133. (b) Yao, C.-J.; Zhong, Y.-W.; Yao, J. *J. Am. Chem. Soc.* **2011**, *133*, 15697. (c) Yao, C.-J.; Sui, L.-Z.; Xie, H.-Y.; Xiao, W.-J.; Zhong, Y.-W.; Yao, J. *Inorg. Chem.* **2010**, *49*, 8347. (d) Wang, L.; Yang, W.-W.; Zheng, R.-H.; Shi, Q.; Zhong, Y.-W.; Yao, J. *Inorg. Chem.* **2011**, *50*, 7074.
(10) (a) Costuas, K.; Rigaut, S. *Dalton Trans.* **2011**, *40*, 5643. (b) Kaim, W. *Inorg. Chem.* **2011**, *50*, 9752.
(11) (a) Nemykin, V. N.; Rohde, G. T.; Barrett, C. D.; Hadt, R. G.; Bizzarri, C.; Galloni, P.; Floris, B.; Nowik, I.; Herber, R. H.; Marrani, A. G.; Zanoni, R.; Loim, N. M. *J. Am. Chem. Soc.* **2009**, *131*, 14969. (b) Glauser, R.; Hauser, U.; Herren, F.; Ludi, A.; Roder, P.; Schmidt, E.; Siegenthaler, H.; Wenk, F. *J. Am. Chem. Soc.* **1973**, *95*, 8457. (c) Felix, F.; Ludi, A. *Inorg. Chem.* **1978**, *17*, 1782.
(12) (a) Hankache, J.; Wenger, O. S. *Chem. Rev.* **2011**, *111*, 5138. (b) Heckmann, A.; Lambert, C. *Angew. Chem., Int. Ed.* **2012**, *51*, 326.
(13) (a) Biswas, R.; Mukherjee, S.; Kar, P.; Ghosh, A. *Inorg. Chem.* **2012**, *51*, 8150. (b) Meyer, F.; Demeshko, S.; Leibeling, G.; Kersting, B.; Kaifer, E.; Pritzkow, H. *Chem.—Eur. J.* **2005**, *11*, 1518. (c) Woodard, B.; Willett, R. D.; Haddad, S.; Twamley, B.; Gomez-Garcia, C. J.; Coronado, E. *Inorg. Chem.* **2004**, *43*, 1822. (d) Escuer, A.; Aromí, G. *Eur. J. Inorg. Chem.* **2006**, 4721.
(14) (a) Ni, Z.-H.; Kou, H.-Z.; Zheng, L.; Zhao, Y.-H.; Zhang, L.-F.; Wang, R.-J.; Cui, A.-L.; Sato, O. *Inorg. Chem.* **2005**, *44*, 4728. (b) Karmakar, T. K.; Ghosh, B. K.; Usman, A.; Fun, H.-K.; Rivière, E.; Mallah, T.; Aromí, G.; Chandra, S. K. *Inorg. Chem.* **2005**, *44*, 2391.
(15) (a) Mautner, F. A.; Hanna, S.; Cortés, R.; Lezama, L.; Barandika, M. G.; Rojo, T. *Inorg. Chem.* **1999**, *38*, 4647. (b) Naiya, S.; Biswas, S.; Drew, M. G. B.; Gómez-García, C. J.; Ghosh, A. *Inorg. Chem.* **2012**, *51*, 5332.
(16) Dori, Z.; Ziolo, R. F. *Chem. Rev.* **1973**, *73*, 247.
(17) Huynh, M. H. V.; Meyer, T. J.; Labouriau, A.; Morris, D. E.; White, P. S. *J. Am. Chem. Soc.* **2003**, *125*, 2828.
(18) (a) Shiu, K.-B.; Guo, W.-N.; Chan, T.-J.; Wang, J.-C.; Liou, L.-S.; Peng, S.-M.; Cheng, M.-C. *Organometallics* **1995**, *14*, 1732. (b) Govindaswamy, P.; Yennawar, H. P.; Kollipara, M. R. *J. Organomet. Chem.* **2004**, *689*, 3108. (c) Israelson, A.; Zilberberg, N.; Shoshan-Barmatz, V. *Nat. Protoc.* **2006**, *1*, 111. (d) Singh, K. S.; Svitlyk, V.; Devi, P.; Mozharivskyj, Y. *Inorg. Chim. Acta* **2009**, *362*, 5252.
(19) Bai, L.-X.; Han, W.; Wang, W.-Z.; Liu, X.; Yan, S.-P.; Liao, D.-Z. *Acta Crystallogr.* **2004**, *E60*, m953.
(20) Catalano, V. J.; Craig, T. J. *Inorg. Chem.* **2003**, *42*, 321.
(21) Lubben, M.; Meetsma, A.; Wilkinson, E. C.; Feringa, B.; Que, L., Jr. *Angew. Chem., Int. Ed. Engl.* **1995**, *34*, 1512.
(22) Kojima, T.; Weber, D. M.; Choma, C. T. *Acta Crystallogr.* **2005**, *E61*, m226.
(23) Ohzu, S.; Ishizuka, T.; Hirai, Y.; Jiang, H.; Sakaguchi, M.; Ogura, T.; Fukuzumi, S.; Kojima, T. *Chem. Sci.* **2012**, *3*, 3421.
(24) Kabuto, C.; Akine, S.; Nemoto, T.; Kwon, E. *J. Cryst. Soc. Jpn.* **2009**, *51*, 218.
(25) (a) Sheldrick, G. M. *Acta Crystallogr.* **2008**, *A64*, 112. (b) Sheldrick, G. M. *SIR97 and SHELX97, Programs for Crystal Structure Refinement*; University of Göttingen: Göttingen, Germany, 1997.
(26) van der Sluis, P.; Spek, A. L. *Acta Crystallogr.* **1990**, *A46*, 194.
(27) See the SI.
(28) The asymmetric units of the single crystal of **1** and $[Ru^{II}(N4Py)(NCCH_3)](PF_6)_2$ involved two independent cation parts, and thus the value mentioned in the text is the mean value of the corresponding values of the two independent cations.
(29) Huheey, J. E.; Keiter, E. A.; Keiter, R. L. *Inorganic Chemistry: Principles of Structure and Reactivity*, 4th ed.; Harper Collins College Publishers: New York, 1993; pp 543−545.
(30) Although the Ru−N1 length of **2** [2.020(10) Å] is relatively shorter than that of **1**, the standard deviations of the structural data for **2** are relatively large because of the low quality of the crystal. Therefore, a detailed discussion on the bond lengths for **2** was difficult.
(31) (a) Seok, W. K.; Yim, S. B.; Klapötke, T. M.; White, P. S. *J. Organomet. Chem.* **1998**, *559*, 165. (b) Fukui, S.; Kajihara, A.; Hirano, T.; Sato, F.; Suzuki, N.; Nagao, H. *Inorg. Chem.* **2011**, *50*, 4713.
(32) (a) Kim, N.-K.; Chang, K.-J.; Moon, D.; Lah, M. S.; Jeong, K.-S. *Chem. Commun.* **2007**, 3401. (b) Kang, S. O.; Day, V. W.; Bowman-James, K. *Inorg. Chem.* **2010**, *49*, 8629.
(33) (a) Clementi, E.; McLean, A. D. *J. Chem. Phys.* **1963**, *39*, 323. (b) Rossi, A. R.; Bartram, R. H. *J. Chem. Phys.* **1979**, *70*, 532.
(34) Stretching bands due to N_3^- ligands of ruthenium complexes have been reported to be observed in the range of 2015−2030 cm^{-1}. (a) Sellmann, D.; Gottschalk-Gaudig, T.; Heinemann, F. W. *Inorg. Chim. Acta* **1998**, *269*, 63. (b) Kimura, T.; Arita, H.; Ishiwata, K.; Kuwata, S.; Ikariya, T. *Dalton Trans.* **2009**, 2912.
(35) (a) Kane-Maguire, L. A. P.; Sheridan, P. S.; Basolo, F.; Pearson, R. G. *J. Am. Chem. Soc.* **1970**, *92*, 5865. (b) Jüstel, T.; Bendix, J.; Metzler-Nolte, N.; Weyhermüller, T.; Nuber, B.; Wieghardt, K. *Inorg. Chem.* **1998**, *37*, 35−43. (c) Matsumura, S.; Shikano, K.; Oi, T.; Suzuki, N.; Nagao, H. *Inorg. Chem.* **2008**, *47*, 9125.
(36) Díez, Á.; Forniés, J.; Larraz, C.; Lalinde, E.; López, J. A.; Martín, A.; Moreno, M. T.; Sicilia, V. *Inorg. Chem.* **2010**, *49*, 3239.
(37) (a) Duati, M.; Tasca, S.; Lynch, F. C.; Bohlen, H.; Vos, J. G.; Stagni, S.; Ward, M. D. *Inorg. Chem.* **2003**, *42*, 8377. (b) Yang, W.-W.; Zhong, Y.-W.; Yoshikawa, S.; Shao, J.-Y.; Masaoka, S.; Sakai, K.; Yao, J.; Haga, M. *Inorg. Chem.* **2012**, *51*, 890.
(38) (a) Kojima, T.; Hayashi, K.; Matsuda, Y. *Inorg. Chem.* **2004**, *43*, 6793. (b) Kojima, T.; Noguchi, D.; Nakayama, T.; Inagaki, Y.; Shiota, Y.; Yoshizawa, K.; Ohkubo, K.; Fukuzumi, S. *Inorg. Chem.* **2008**, *47*, 886.
(39) When we measured the CV and DPV of **2** at a faster scan rate (5 V s^{-1}) in CH_3CN at −40 °C, the reversibility of the second redox wave was slightly improved (Figure S7 in the SI).
(40) Connelly, N. G.; Geiger, W. E. *Chem. Rev.* **1996**, *96*, 877.
(41) (a) Małecki, J. G.; Maroń, A. *Polyhedron* **2012**, *31*, 44. (b) Krause, R. A.; Krause, K. *Inorg. Chem.* **1982**, *21*, 1714.
(42) Because of the ill electrochemical reversibility of the second redox process of **2**, the addition of 2 equiv of the oxidant was not enough to complete the two-electron oxidation of **2** (Figure S8 in the SI).
(43) (a) Brown, G. M.; Callahan, R. W.; Meyer, T. J. *Inorg. Chem.* **1975**, *14*, 1915. (b) Ho, C.-M.; Leung, H.-C.; Wu, S.; Low, K.-H.; Lin, Z.; Che, C.-M. *Eur. J. Inorg. Chem.* **2012**, 151.
(44) Hush, N. S. *Coord. Chem. Rev.* **1985**, *64*, 135.
(45) Recently, most of MV complexes of a metal−ligand−metal type have been revealed to obey a three-state electronic model: (a) Launay, J.-P.; Coudret, C.; Hortholary, C. *J. Phys. Chem. B* **2007**, *111*, 6788. (b) Lambert, C.; Nöll, G.; Schelter, J. *Nat. Mater.* **2002**, *1*, 69. Herein,

we analyzed the MV properties of **2** on the basis of a classical two-state model.
(46) Richardson, D. E.; Taube, H. *J. Am. Chem. Soc.* **1983**, *105*, 40.
(47) Tom, G. M.; Taube, H. *J. Am. Chem. Soc.* **1975**, *97*, 5310.
(48) Richardson, D. E.; Sen, J.; Buhr, J. D.; Taube, H. *Inorg. Chem.* **1982**, *21*, 3136.
(49) We reported the K_C value of **8** previously: Kojima, T.; Amano, T.; Ishii, Y.; Ohba, M.; Okaue, Y.; Matsuda, Y. *Inorg. Chem.* **1998**, *37*, 4076 . In this work, we detected the IVCT absorption band in CH_3CN upon one-electron oxidation of **8** with 1 equiv of TBAH at room temperature as shown in Figure S9 (SI).
(50) Baitalik, S.; Flörke, U.; Nag, K. *J. Chem. Soc., Dalton Trans.* **1999**, 719.
(51) (a) Ceccon, A.; Santi, S.; Orian, L.; Bisello, A. *Coord. Chem. Rev.* **2004**, *248*, 683. (b) Yang, W.-W.; Yao, J.; Zhong, Y.-W. *Organometallics* **2012**, *31*, 8577.
(52) (a) Adhikary, C.; Koner, S. *Coord. Chem. Rev.* **2010**, *254*, 2933. (b) Escuer, A.; Vlahopoulou, G.; Mautner, F. A. *Inorg. Chem.* **2011**, *50*, 2717. (c) Jia, Q.-X.; Tian, H.; Zhang, J.-Y.; Gao, E.-Q. *Chem.—Eur. J.* **2011**, *17*, 1040. (d) Liu, F.-C.; Zeng, Y.-F.; Zhao, J.-P.; Hu, B.-W.; Ribas, J.; Cano, J. *Inorg. Chem.* **2007**, *46*, 1520.